Proceedings for the 2018 EUMETSAT Meteorological Satellite Conference, 17-21 September 2018, Tallinn, Estonia

IMPROVED LUNAR EDGE RESPONSE FUNCTION FOR ON-ORBIT MTF CALIBRATION USING ALBEDO LUNAR FLATTENING

Dr. James N. Caron and Dr. Chris Rollins

Research Support Instruments, 4325-B Forbes Boulevard, Lanham, MD, 20706 USA

Abstract

Modulation transfer functions (MTF) are measured from images to quantify the resolution performance of the imaging system. A common approach is to capture an image of an edge feature in the scene and then derive a one-dimensional line spread function whose normalized Fourier Transform is the one-dimensional modulation transfer function. Finding an appropriate edge feature can be difficult for satellite-based Earth-sensing cameras. Research groups have imaged naturally occurring edges while others have created edge features by placing large tarpaulins in the scene, but imaging through the turbulent atmosphere complicates the measurement. The recorded MTF becomes a function of both the optical system and the propagation of the light through the turbulent atmosphere. An alternative approach is to image the sharp edge of the Moon as it is illuminated by the Sun. The Moon's surface, however, has features, e.g. craters and seas, that depart from clean step-like behavior at the edge, diminishing the effectiveness of the method. In this paper, we demonstrate an improvement in this method where a reflectance (albedo) map of the Moon, created from a mosaic of DoD/NASA Clementine images, is used to flatten the surface features of the Moon before the Edge Spread Function is measured. The objective is to improve the reliability of MTF measurements for on-orbit calibration of the NASA GOES weather satellites and similar missions.

INTRODUCTION

Measuring the edge spread function (ESF) of an optical system is a conventional method to derive the modulation transfer function (MTF) of the imaging system. (International Standard ISO 12233:2017) This is accomplished in a laboratory setting by imaging a scene with a distinct line feature, positioned such that the edge is neither parallel or perpendicular to the image axes. The spatial derivative of the edge feature is used to calculate the MTF of the system. [11] This diagnostic is difficult to apply when the imaging system is orbiting the Earth. Several groups, such as [6] and [8], have imaged edge features on the Earth to estimate the MTF, but imaging through the turbulent atmosphere complicates the measurement. The recorded MTF becomes a function of both the optical system and the propagation of the light through the atmosphere.

Atmospheric effects can be avoided by pointing the orbiting camera system to the moon and imaging the illuminated lunar edge. This ensures a sharp edge with a large brightness contrast between the lunar disk and surrounding space. In 1999, Shea et al. [13] used this method to derive an MTF in the vertical and horizontal directions for the NASA GOES N/O mission. The resulting MTF was used as input for deconvolution of the subsequent images. In 2014, Wang et al. [14] used this technique to monitor the performance of the MODerate resolution Imaging Spectroradiometer (MODIS) onboard the Terra and Aqua satellites. In both cases, the edge of the moon was sufficiently sharp, but features, mainly seas and craters, that depart from clean step-like behavior at the edge, diminishing the effectiveness of the method. An improved measurement can be achieved if the effect of the features can be diminished in post-processing while not impacting the MTF measurement.

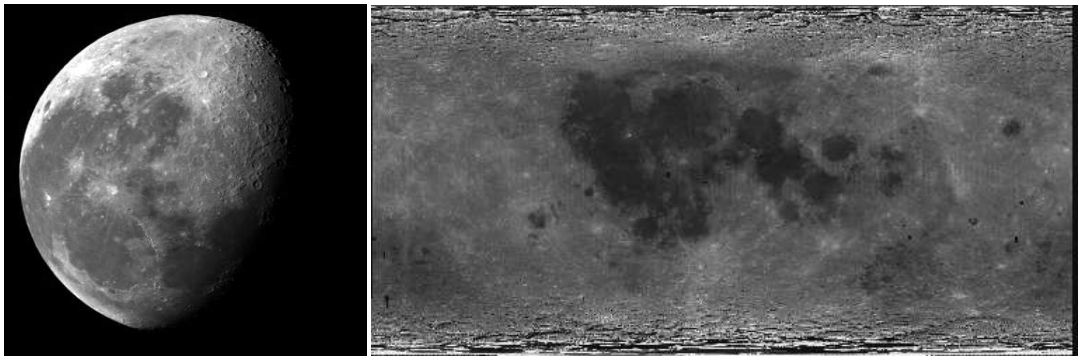

Figure 1: **(Top) Example of an ABI image, taken on February 17, 2017. The moon image is elliptical due to the scan rate of the sensor as it sweeps across the moon. (Bottom) The reflectance (albedo) map assembled from images taken by the DoD/NASA Clementine probe in 1994.**

In this paper, we use a reflectance (albedo) map of the moon, assembled from DoD/NASA Clementine images, [9] to flatten the features of a lunar image captured by the GOES-16 Advanced Baseline Imager (ABI) imager. [12] The Albedo Lunar Flattening (ALF) process involves aligning and projecting the reflectance map to match the target image. Division of the ABI image by the projected Clementine image produces a featureless moon that can be used for the ESF measurement.

REPRESENTATIVE IMAGES

Launched on November 19, 2017, GOES-16 is a NOAA/NASA geosynchronous environmental monitoring satellite. The advanced baseline imager (ABI) is a 16-channel passive imaging radiometer operating as a 1×1460 pixel array that scans across a two-dimensional scene. [12] Images of the moon are taken periodically to provide calibration of the sensors. The ABI image shown in Figure 1 (left) was taken from the first band, wavelength of 0.47 μm, on February 17, 2017, and is used in this paper to demonstrate our technique.

The Clementine lunar mapper launched in 1994 as a joint space venture between the Ballistic Missile Defense Organization and NASA. The high resolution camera consisted of a Thompson CCD and six position filter wheel. A goal of the mission was to obtain multi-spectral images of the entire lunar surface. A reflectance map was created by stitching the images as shown in Figure 1 (right) This is a revised 750 nm mosaic (v. 2.0) created at USGS [5] to refine the locations of component images using the latest geodetic control and projected onto a topographic model of the lunar surface. [1]

Our goal was to use the Clementine reflectance map to diminish the features on the ABI moon in order to improve the MTF measurement. This was accomplished using the following steps:

1. Determine the position and elliptical shape of the moon in the ABI image.
2. Find the coordinates of the reflectance map that correspond to the center of the moon in the ABI image.
3. Determine the rotational difference between the images.
4. Project the radiometric Clementine map to fit ABI image.
5. Correct for interpolation errors and spectral differences to create a quasi-flat field.
6. Divide the quasi-flat field from the ABI image.
7. Assemble edge spread function by aligning several horizontal profile plots along lunar edge near mid point of moon.
8. Use the function fit applied to edge spread function to measure the MTF.

Figure 2: **(Left) Spherical projection of the AHI image. (Right) Spherical projection of the Clementine reflectance map.**

ELLIPTICAL SOLUTION

To facilitate the alignment of the images, the shape, size and location of the ABI moon must be determined. Ideally, these values could be calculated from the scanning rate, position of the moon, satellite, and the field-of-view of the optical system. However these values were not available with sufficient accuracy. As such, an empirical measurement directly from the image is necessary. We took the following steps:

1. Apply Sobel 45 and 135 degree edge detection functions to isolate the lunar rim.
2. Apply a threshold filter to remove outliers and portions of the rim that fall into shadow.
3. Apply a non-linear least squares fitting function to determine the center and semi-axes of the ellipse. [7]
4. The fit results are verified visually by overlaying the calculated ellipse onto the image.

This approach is similar to the ‘alternate’ approach described in reference [14]. With the elliptical solution in hand, the ABI image is stretched in the direction of the minor axis by the ratio of the major axis to the minor axis to form a spherical projection of the moon. This image, shown in Figure 2 (left), now becomes the control image for determining the corresponding pixel (CP) and rotation difference. The spherical projection of the Clementine image is shown in Figure 2 (right).

CORRESPONDING PIXEL AND ROTATION

We seek to find the coordinates in the Clementine map that correspond to the center pixel of the spherically-projected ABI moon. This is complicated by the difference between orientations of the images. As such, both the relative position and rotation differences need to be determined. We employ an iterative process that searches an area to find the coordinates that will produce the best correspondence. The process takes a few hours on a desktop computer and has the following steps:

1. Through visual inspection, roughly locate the center of the ABI image in the Clementine image, designated the corresponding pixel (CP), by identifying similar lunar features.
2. Define a search area (typically 64 by 64 pixels) around the best guess of the CP.
3. For each pixel in the search area, project the cylindrical Clementine image into a sphere and use log-polar phase correlation [10] to compare the image to the spherical ABI image. The correlation peak location provides information about the amount of rotation and scale difference between the images. The correlation peak amplitude provides the level of confidence in the match.

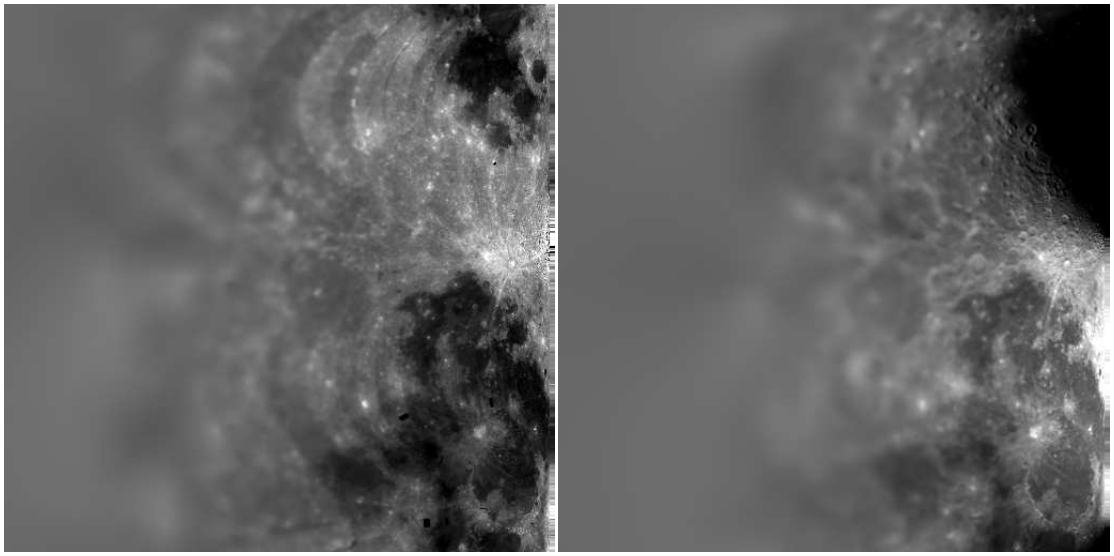

Figure 3: **Log-polar transformations of the spherical Clementine image (left) and the spherical ABI image (right). Vertical axis is rotation and horizontal axis is scale.**

4. Map the correlation peak amplitude and calculated rotation for each pixel in the search area.
5. Identify the location of the maximum value in the correlation peak map to sub-pixel accuracy using a centroid. This is the CP, which can be expressed by pixel index or selenographic coordinates.
6. The rotation can be found by re-calculating the log-polar phase correlation for the CP location, or using an interpolation on the rotation map.

Phase Correlation

Phase Correlation is an established method that determines the translational differences between images. [10] Given two images, $I_c(x, y)$ and $I_t(x, y)$, that differ only by a translation $I_t(x, y) = I_c(x - \Delta x, y - \Delta y)$ the Fourier transforms of those images are related by

$$F_t(u, v) = e^{-i(\Delta x\ u + \Delta y\ v)} F_c(u, v) \tag{1}$$

where (u, v) are the coordinates in frequency space. Thus, translations in image space appear as phase changes in frequency space and can be isolated using

$$e^{(\Delta x\ u + \Delta y\ v)} = \frac{F_c(u, v) F_t^*(u, v)}{|F_c(u, v) F_t^*(u, v)|} \tag{2}$$

where $*$ represents the complex conjugate. Application of a Fourier transform to the phase difference between translated images ideally contains a delta function centered at the displacement coordinates. The $\hat{x}$ and $\hat{y}$ distances from this point to the center of the image are equal to the translation errors. A centroid of the surrounding pixels finds the sub-pixel location. [2]

To achieve measurement of rotation (and scale if desired) difference, the image is re-mapped, in image space, such that the vertical axis represents the angle θ of the pixel coordinates, and the horizontal axis represents the radius ρ of the pixel coordinates. Performing the phase correlation on $I_C(\rho, \theta)$ and the target image $I_T(\rho, \theta)$ would produce a correlation peak whose location represents the rotation and magnification of the image. Figure 3 shows the log-polar transformation of the spherical Clementine image (left) and the ABI image (right). Note that there is a sizable area in the polar ABI image that does not contain information as a result of the moon's shading. The phase correlation method is very tolerant of missing data.

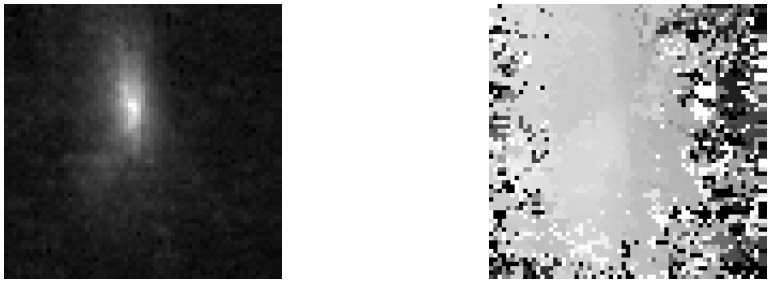

Figure 4: **A 46 by 64 correlation peak map (left) and rotation map (right) produced by performing a rotational phase correlation between the spherical Clementine image and AHI image over the search area.**

Figure 5: **(Left) The Band 1 ABI Lunar image. (Right) The image after division by a correction image created from the Clementine reflectance map.**

The correlation peak amplitude is recorded for every pixel of the search area producing a correlation map, as shown in Figure 4 (left). For each location, there is a corresponding rotation, Figure 4 (right), and scale difference. To find the corresponding pixel, the maximum value is located in the correlation map using a centroid to achieve sub-pixel accuracy.

Spectral And Interpolation Correction

There is a difference in the spectral range of the Clementine image, centered at 750 nm, and the ABI image, centered at 481 nm. The difference primarily affects the processing of the crater regions which appear darker when the ABI wavelength is lower than the Clementine image. This affect can be corrected by applying a gamma function in the form of $I(m,n)^{\gamma}$ to the Clementine projection. For each ABI band, the applied gamma variation is determined by trial-and-error to achieve diminished features with respect to surrounding areas.

Using the final values for rotation and CP, the Clementine image is projected to sphere, and then scaled to match the elliptical ABI image. Limiting geometric operations to the Clementine image ensures that the ABI image will not be influenced by the geometric interpolations. Interpolation of the Clementine image, however, can produce errors at the lunar edge, where there is no information. To compensate for this issue, an image is created that has the dimensions of the Clementine image, but with pixel values set to unity. All operations that are applied to the Clementine image are also

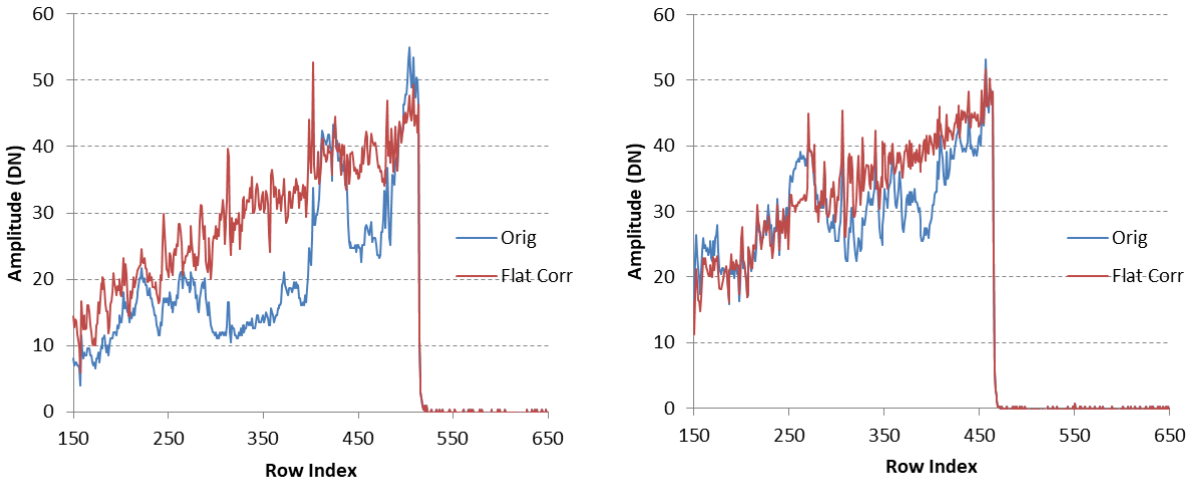

Figure 6: **Representative profile plots from an original ABI image (blue) and the albedo-corrected image (red).**

applied to this 'white' image. Pixels on this white image are unaffected by the interpolations with the exception of diminished values along the elliptical rim. The Clementine projection is divided by this correction image to produce the Clementine albedo flat-field.

RESULTS

The original ABI image is divided by the Clementine albedo flat-field to reduce the large-scale features of the moon as shown in Figure 5. Owing to the difference in spatial resolutions of the images, small-scale features are still visible. The effectiveness can be seen in profile plots taken from the edge of the image to the center. The plots, shown in Figure 6, compare the original and processed images further demonstrating the removal of large scale features.

Edge Spread Functions

The next step is to find the edge spread function (ESF) from the corrected ABI image. Since these already images possess good resolution, there are very few pixels that define the edge for a single row. When applying a line-out, this would be insufficient data points to produce an accurate ESF. Alternatively, we can combine several rows to increase the number of data points. The rows must be shifted such that the edge position in each row is aligned with sub-pixel accuracy. This is accomplished by fitting an edge function to each row in order to obtain the position of the edge with great accuracy. We multiplied a Sigmoid function with a ramp to produce

$$F(x) = [a_0 x + a_1]\left(1 - \frac{1}{1 + \exp(-a_3(x - a_2))}\right) \tag{3}$$

where the first function is a linear equation with a slope a_0 and offset a_1, describing the shading. The second function is the Sigmoid fit where a_2 gives the position of the edge and a_3 gives a value related to the curve.

The a_2 parameter is used to align sequential rows in order to populate a single data set from multiple rows. A final fit of equation 3 is applied to derive a continuous curve from the data points to serve as the edge spread function. Figure 7 (left) shows the alignment of 16 rows near the center of the moon. For accurate MTF measurements, this technique should be applied to the middle rows to

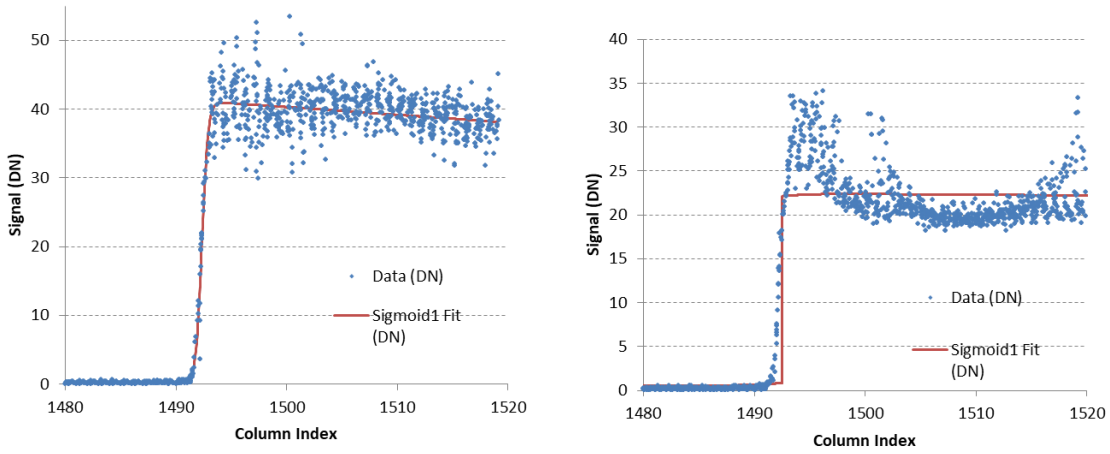

Figure 7: **(Left) Alignment and fit to 16 rows near the image equator for Band 1 on the albedo-flattened image. Applying the same procedure to the original ABI produces the data and fit on the right.**

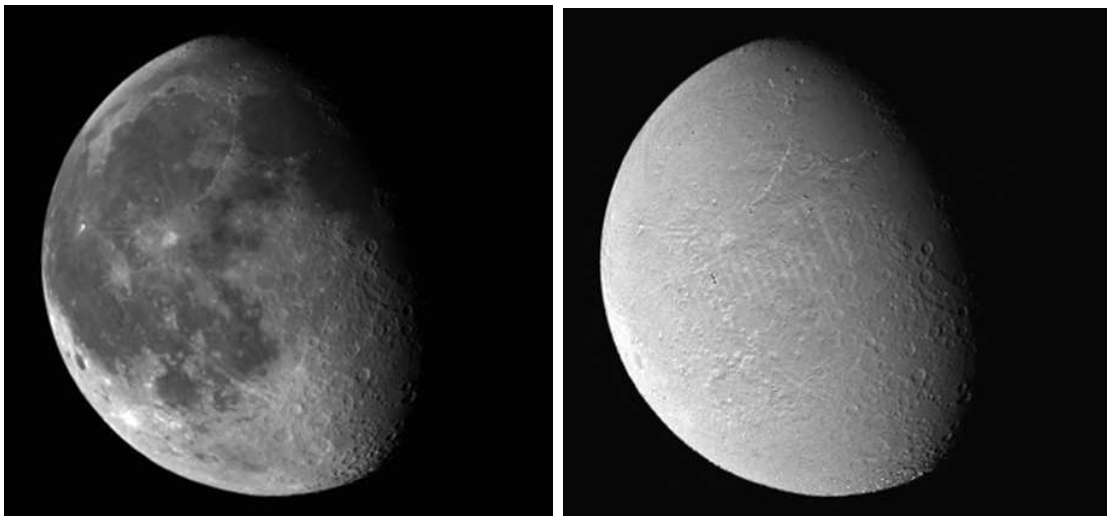

Figure 8: **Application of ALF to the third channel ($\lambda = 0.87\ \mu m$) of the ABI imager.**

diminish the effects of aliasing. The data shows some outlier values that are the result of moon features, but there is sufficient data to establish a good fit. For comparison, the same process was applied to the image before the division by the albedo correction. The fit, shown in Figure 7 (right), obviously fails. The line spread function is created by taking the derivative of the ESF with the ramp removed. The MTF is calculated by taking the magnitude of the FFT of the line spread function.

CONCLUSION

We have presented the Albedo Lunar Flattening method to improve MTF measurements where an edge response function is derived from the lunar edge. A reflectance (albedo) map from the Clementine mission was aligned to an image of the moon taken by the NASA GOES-16 satellite using repeated applications of polar phase correlation to obtain both the difference in location and rotation. The Clementine image was re-mapped to act as a flat-field image. Division of the original image by the Clementine correction image effectively removed large-scale features from the ABI image producing an improved measurement of the optical system MTF. This can be achieved for

all non-emissive bands, as demonstrated in Figure 8. The method is an improvement over ground-based calibration in that Earth's atmosphere does not play a role. [3, 4] The method is superior to the previous state-of-the-art [14] since the method diminishes large-scale moon features that could adversely affect the establishment of an edge spread function.

ACKNOWLEDGMENT

This study was supported through the NASA GOES-R Program, ABI Flight Project. The authors would like to thank Dr. F. Weng and Dr. T. Zhu of the GOES-R CWG Proxy Data Team for providing the GOES 16 data. The contents are solely the findings of the authors and do not constitute a statement of policy, decision, or position on behalf of NOAA, NASA or the U.S. Government.

References

[1] Archinal, B.A., M.R. Rosiek, R.L. Kirk, and B.L. Redding. (2006) "A Clementine Derived Control Network and Topographic Model-The Unified Lunar Control Network 2005," In *IAU Joint Discussion*, vol. **10**, p. 26.

[2] Caron, J. N., M. J. Montes, and J. L. Obermark, (2016). "Extracting flat-field images from scene-based image sequences using phase correlation." *Review of Scientific Instruments*, 87(6), 063710.

[3] Hwang, H., Y.-W. Choi, S. Kwak, M. Kim, and W. Park, (2008) "MTF assessment of high resolution satellite images using ISO 12233 slanted-edge method," In *SPIE Remote Sensing*, pp. 710905-710905.

[4] Viallefont-Robinet, F., and D. Léger, (2010) "Improvement of the edge method for on-orbit MTF measurement." *Optics express* **18**, no. 4, pp 3531-3545.

[5] Lee, E.M., L.R. Gaddis, L. Weller, J.O. Richie, T. Becker, J. Shinaman, M.R. Rosiek, and B.A. Archinal, USG, (2009), "A New Clementine Basemap of the Moon," *Lunar and Planetary Science Conference XL*, Houston, TX.

[6] Li, J., F. Xing, T. Sun, and Z. You, (2015) "Efficient assessment method of on-board modulation transfer function of optical remote sensing sensors," *Optics Express* 23, no. 5, pp 6187-6208.

[7] Markwardt, Craig B. (2009) "Non-linear least squares fitting in IDL with MPFIT," ArXiv preprint arXiv:0902.2850.

[8] Nelson, N. R., and P. S. Barry, (2001) "Measurement of Hyperion MTF from on-orbit scenes," In *Geoscience and Remote Sensing Symposium*, IGARSS'01. IEEE 2001 International, vol. **7**, pp. 2967-2969.

[9] Nozette, S., P. Rustan, L. P. Pleasance, J. F. Kordas, I. T. Lewis, H. S. Park, R. E. Priest, D. M. Horan, P. Regeon, C. L. Lichtenberg, E. M. Shoemaker, E. M. Eliason, A. S. McEwen, M. S. Robinson, P. D. Spudis, C. H. Acton, B. J. Buratti, T. C. Duxbury, D. N. Baker, B. M. Jakosky, J. E. Blamont, M. P. Corson, J. H. Resnick, C. J. Rollins, M. E. Davies, P. G. Lucey, E. Malaret, M. A. Massie, C. M. Pieters, R. A. Reisse, R. A. Simpson, D. E. Smith, T. C. Sorenson,R. W. Vorder Breugge, and M. T. Zuber, (1994) "The Clementine mission to the Moon: Scientific overview," *Science* **266**, no. 5192, pp 1835-1839.

[10] Reddy, B. Srinivasa, and Biswanath N. Chatterji, (1996) "An FFT-based technique for translation, rotation, and scale-invariant image registration," *IEEE transactions on image processing* **5**, no. 8, pp 1266-1271.

[11] Reichenbach, S. E., S. K. Park, and R. Narayanswamy, (1991) "Characterizing digital image acquisition devices," *Optical Engineering* **30**, no. 2, pp 170-177.

[12] Schmit, T. J., Paul Griffith, Mathew M. Gunshor, Jaime M. Daniels, Steven J. Goodman, and William J. Lebair. (2017) "A Closer Look at the ABI on the GOES-R Series," *Bulletin of the American Meteorological Society* 98, no. 4, pp 681-698.

[13] Shea, J.J. (1999) "Lunar limb knife-edge optical transfer function measurements," *J. Electron. Imaging.* 0001;8(2):196-208.

[14] Wang, Z., X. Xiong, T. Choi, and D. Link, (2014) "On-Orbit Characterization of MODIS Modulation Transfer Function Using the Moon," IEEE Transactions On Geoscience And Remote Sensing **52**, no. 7, pp 4112-4121.